Microbiology (2009), **155**, 2116–2126 **DOI** 10.1099/mic.0.027706-0

Actinomyces naeslundii in initial dental biofilm formation

I. Dige,[1] M. K. Raarup,[2] J. R. Nyengaard,[2] M. Kilian[3] and B. Nyvad[1]

Correspondence
Irene Dige
idige@odont.au.dk

[1]Department of Dental Pathology, Operative Dentistry and Endodontics, School of Dentistry, Aarhus University, Vennelyst Boulevard 9, 8000 Aarhus C, Denmark

[2]Stereology and Electron Microscopy Research Laboratory and MIND Center, Aarhus University, Ole Worms Allé 8, 8000 Aarhus C, Denmark

[3]Department of Medical Microbiology and Immunology, Aarhus University, Wilhelm Meyers Allé 4, 8000 Aarhus C, Denmark

Received 4 February 2009
Revised 31 March 2009
Accepted 27 April 2009

The combined use of confocal laser scanning microscopy (CLSM) and fluorescent *in situ* hybridization (FISH) offers new opportunities for analysis of the spatial relationships and temporal changes of specific members of the microbiota of intact dental biofilms. The purpose of this study was to analyse the patterns of colonization and population dynamics of *Actinomyces naeslundii* compared to streptococci and other bacteria during the initial 48 h of biofilm formation in the oral cavity. Biofilms developed on standardized glass slabs mounted in intra-oral appliances worn by ten individuals for 6, 12, 24 and 48 h. The biofilms were subsequently labelled with probes against *A. naeslundii* (ACT476), streptococci (STR405) or all bacteria (EUB338), and were analysed by CLSM. Labelled bacteria were quantified by stereological tools. The results showed a notable increase in the number of streptococci and *A. naeslundii* over time, with a tendency towards a slower growth rate for *A. naeslundii* compared with streptococci. *A. naeslundii* was located mainly in the inner part of the multilayered biofilm, indicating that it is one of the species that attaches directly to the acquired pellicle. The participation of *A. naeslundii* in the initial stages of dental biofilm formation may have important ecological consequences.

INTRODUCTION

Dental biofilm is an archetypal example of a complex biofilm (Costerton *et al.*, 1999; Davies, 2003; DuPont, 1997). Biofilm formation on tooth surfaces follows the same basic rules as biofilm formation elsewhere in nature. Dental biofilms develop readily because of the optimal temperature, the rich nutrient supply in the oral cavity, and the hard non-shedding surface. They are easily accessible for experimentation using intra-oral devices (Auschill *et al.*, 2004; Kilian *et al.*, 1979; Nyvad & Fejerskov, 1987a; Palmer *et al.*, 2003), and therefore dental biofilms can be used to demonstrate colonization phenomena and ecological principles of universal interest. Concurrent with the increasing recognition of the significance of biofilms in infectious diseases, the development of techniques such as confocal laser scanning microscopy (CLSM), fluorescence *in situ* hybridization (FISH) and immunofluorescence has enabled visualization of bacteria in their natural undisturbed environment. This offers a substantial improvement upon previous microbiological studies of bacteria grown in planktonic settings (Anwar *et al.*, 1992; Davies, 2003).

Previous studies of dental biofilm that took advantage of these methods mainly focused on streptococci (Diaz *et al.*, 2006; Dige *et al.*, 2007; Hannig *et al.*, 2007; Palmer *et al.*, 2003) because culture-based studies suggested that this group of bacteria is prominent during the initial stages of biofilm formation on teeth (Li *et al.*, 2004; Nyvad & Kilian, 1987, 1990). However, other genera such as *Actinomyces* are also among the earliest colonizers of dental surfaces and may constitute up to 27 % of the pioneer bacteria (Kilian *et al.*, 1979; Li *et al.*, 2004; Nyvad & Kilian, 1987). Several culture-based studies indicated that *Actinomyces* species gain increased prominence at the expense of streptococci during maturation of the biofilm (Ritz, 1967; Socransky *et al.*, 1977; Syed & Loesche, 1978; van Palenstein Helderman, 1981). Such population changes might reflect differences in growth rates (Nyvad & Kilian, 1987; Socransky *et al.*, 1977) and/or differences in nutritional profiles of these genera (Takahashi *et al.*, 1995; Takahashi & Yamada, 1996; van der Hoeven & van den Kieboom, 1990; Yaling *et al.*, 2006). However, the spatial relationship of actinomycetes with other members of the dental biofilm microbiota was not disclosed by these culture-based studies.

Abbreviations: CLSM, confocal laser scanning microscopy; FISH, fluorescent *in situ* hybridization.

A supplementary figure is available with the online version of this paper.

Previous transmission electron microscopic studies consistently showed the presence of densely packed colonies of pleomorphic Gram-positive bacteria resembling *Actinomyces* in contact with the tooth surface in young and mature supragingival plaque (Listgarten *et al.*, 1975; Nyvad & Kilian, 1987; Schroeder & De Boever, 1970), and similar morphotypes were observed in the demineralized dentine of root surface caries (Nyvad & Fejerskov, 1989). Due to methodological limitations it was not possible at that time to verify the identity of these bacteria. In a recent study using combined CLSM and FISH analysis *Actinomyces naeslundii* constituted up to 18 % of the microbiota within the first days of dental biofilm formation, with a notable decrease over the 7 day observation period (Al-Ahmad *et al.*, 2007). Direct imaging of *A. naeslundii* during sequential stages of the initial colonization of hard dental surfaces is still lacking. Such information is important for understanding the role of *A. naeslundii* during initial biofilm development as well as its ecological role in dental disease processes.

The aims of this study were therefore to describe the pattern of colonization and to analyse population dynamics of *A. naeslundii* compared to that of streptococci and other bacteria, during the initial 6–48 h of dental biofilm formation.

METHODS

Experimental conditions. Oral biofilms were collected on custom-made glass slabs (Menzel). The glass slabs were industrially manufactured ($4 \times 4 \times 1$ mm) with a surface roughness of 1200 grit. Six glass slabs were mounted slightly recessed in the buccal flanges of individually designed intra-oral appliances worn by ten healthy volunteers (five females and five males, 23–36 years of age, median age 25 years) for 6, 12, 24 and 48 h. The volunteers retained the appliance intra-orally throughout the experimental period, except during tooth brushing and intake of food or liquids other than water. The Ethics Committee of Aarhus County approved the protocol, and informed consent was obtained from all participants after they received oral and written instructions about the study. A detailed description of the experimental model and the experimental conditions has been previously published (Dige *et al.*, 2007).

Specimen preparation

FISH. Following *in situ* biofilm growth, FISH was performed as described by Dige *et al.* (2007), using specific 16S rRNA probes against streptococci, *A. naeslundii* and all bacteria. Immediately after removal from the oral cavity, the glass slabs with the biofilms were fixed in 4 % paraformaldehyde (3 vols) in PBS (1 vol.) (Stahl & Amann, 1991) for 3 h at 4 °C. The specimens were subsequently washed with sterile PBS and stored in a mixture of 100 % ethanol and PBS (1 : 1) at −20 °C. For permeabilization, the glass slabs with the biofilm were mounted on diagnostic glass microscope slides (Menzel) with paraffin wax (GC Corporation) and treated with 25 µl lysozyme (Sigma) [70 U μl^{-1} in 100 mM Tris/HCl pH 7.5 (Sigma), 5 mM EDTA (Merck)] for 9 min at 37 °C in a humid chamber. The diagnostic glass microscope slides with the biofilms were then rinsed with ultrafiltrated water, dehydrated in series of ethanol washes (50, 80 and 100 %; 3 min each wash) and dried for 10 min in a vertical position. The glass slabs were then exposed to 10 µl hybridization buffer (0.9 M NaCl, 20 mM Tris/HCl pH 7.5, 0.01 % SDS, 30 % formamide, which pilot studies showed to be the optimal concentration for the probe/label combination used) containing 100 ng of the designated oligonucleotide probe and incubated at 46 °C for 2 h in a humid atmosphere in the dark. After hybridization, the glass microscope slides were first washed in buffer (20 mM Tris/HCl pH 7.5, 5 mM EDTA, 0.01 % SDS and 112 mM NaCl) for 15 min in a water bath at 48 °C, and then rinsed in ice-cold ultrafiltrated water. The oligonucleotide probe STR405 (5′-TAG CCG TCC CTT TCT GGT-3′) (MWG Biotech) labelled with Alexa488 was used to identify all *Streptococcus* spp. (Paster *et al.*, 1998) and the oligonucleotide probe ACT476 (5′-ATC CAG CTA CCG TCA ACC-3′) (IBA) labelled with Atto550 was used to identify *A. naeslundii* (Gmür & Lüthi-Schaller, 2007). The oligonucleotide probe EUB338 (5′-GCT GCC TCC CGT AGG AGT-3′) (IBA) labelled with Atto633 was used as a positive control based on its ability to detect all bacteria (Amann *et al.*, 1990) with a few exceptions such as *Treponema maltophilum* and *Treponema lecithinolyticum* (Daims *et al.*, 1999), which are not involved in the early phase of biofilm formation. A search performed in the Ribosomal Database Project II at http://rdp.cme.msu.edu/index.jsp indicated that the probe EUB338 recognizes 241 803 out of 335 830 bacterial sequences in the database, including all taxa of bacteria hitherto detected in the oral cavity.

Using the above protocol the specificity of the probes used in the study was tested on smears of saline suspensions of the following strains obtained from the National Collection of Type Cultures (NCTC), Colindale, London, UK; the American Type Culture Collection (ATCC), Manassas, VA, USA; and the Culture Collection of the University of Gothenburg (CCUG), Gothenburg, Sweden: *Streptococcus mutans* NCTC 10449^T, *Streptococcus sanguinis* ATCC 10556^T, *Streptococcus gordonii* ATCC 10558^T, *Streptococcus oralis* NCTC 7864^T, *Streptococcus mitis* NCTC 12261^T, *Streptococcus infantis* GTC849^T, *Streptococcus anginosus* NCTC 10713^T, *Streptococcus constellatus* ATCC 27823^T, *Streptococcus intermedius* ATCC 27335^T, *Streptococcus salivarius* NCTC 8618^T, *Streptococcus parasanguinis* CCUG 27742, *Streptococcus cristatus* SK231, *Streptococcus pseudopneumoniae* SK674, *Streptococcus pneumoniae* TIGR4, *Streptococcus sinensis* CCUG 48488^T, *Streptococcus pyogenes* clinical isolate, *Abiotrophia defectiva* SK892, *Gemella haemolysans* CCUG 37985^T, *Globicatella adiacens* SK932, *Enterococcus faecalis* clinical isolate, *Lactobacillus acidophilus* ATCC 4504, *Actinomyces bowdenii* CCUG 37421^T (cat), *Actinomyces cardiffensis* CCUG 44997^T, *Actinomyces funkei* CCUG 42773^T, *Actinomyces georgiae* CCUG 32935^T, *Actinomyces gerencseriae* CCUG 34703^T, *Actinomyces graevenitzii* CCUG 27294^T, *Actinomyces dentalis* CCUG 48064^T, *Actinomyces denticolens* CCUG 32758^T (cattle), *Actinomyces israelii* NCTC 6826^T, *Actinomyces massiliensis* CCUG 53522^T, *Actinomyces meyeri* CCUG 21024^T, *Actinomyces naeslundii* ATCC 12104^T, *A. naeslundii* genomospecies 2 WVU627/75, *Actinomyces odontolyticus* NCTC 9935 and CCUG 20536^T, *Actinomyces oricola* CCUG 46090^T, *Actinomyces radingae* CCUG 34270^T, *Actinomyces viscosus* CCUG 14476^T (rat), *Propionibacterium acnes* ATCC 737, *Rothia dentocariosa* ATCC 14189^T, *Bifidobacterium bifidum* ATCC 15696^T, *Staphylococcus aureus* clinical isolate, *Staphylococcus epidermidis* clinical isolate and *Veillonella parvula* clinical isolate. Except where indicated, these species are all associated with humans. The probe STR405 gave a strong fluorescent reaction with all bacteria in the slides prepared with all *Streptococcus* species. Apart from a very weak staining of *Abiotrophia defectiva*, easily distinguishable from the positive reactions seen with *Streptococcus* species, no other strain gave a positive reaction. The probe ACT476 gave a strong reaction with all bacteria in smears of *Actinomyces naeslundii*, including *A. naeslundii* genomospecies 2, *A. bowdenii*, *A. viscosus* and *A. denticolens*, but no reaction with other *Actinomyces* species or with other bacteria in the test panel. This is in agreement with the complete conservation of the target

sequence in the positive species and single to multiple sequence deviations in the negative species (Fig. 1). Based on these observations it was concluded that probe ACT476 reacts only with *A. naeslundii* among species that are associated with humans. The DAPI reagent stained all bacteria in the panel.

CLSM. The glass slabs with the biofilm were examined on an inverted Zeiss LSM 510 META confocal microscope using 488, 543 and 633 nm laser lines for excitation of Alexa488, Atto550 and Atto633, respectively. Emission bandpass filters were set to 500–530 nm for detection of Alexa488, 565–615 nm for detection of Atto550, and 651–704 nm for detection of Atto633. Images were acquired using a ×63 (NA=1.2) water-immersible objective (C-Apochromat) with a working distance of 0.28 mm and collected at electronic zoom ×0.7 (2048×2048 pixels, pixel size 100 nm=optimum resolution), ×2 (1024×1024 pixels, pixel size 70 nm) and ×4 (1024×1024 pixels, pixel size 30 nm), of which the last was used for quantification. Images were acquired with pinholes set to 1 Airy unit, corresponding to an optical slice thickness of 1.0 μm. Prior to microscopy the glass slabs with the biofilms were mounted on a plastic device so that the biofilm could be turned upside down in a chambered coverglass for examination by the inverted microscope. A drop of Citifluor AF3 anti-bleaching reagent was applied between the biofilm and the chambered coverglass. For the qualitative analysis each biofilm was scanned at representative areas, avoiding the edges of the glass slabs. *z* series of optical sections were generated by vertical sectioning at 1 μm distances through the biofilm. Because the surface was never exactly horizontal with respect to the microscope stage, the number of optical sections per specimen was not directly translatable to biofilm thickness. For quantitative analysis (zoom 4) each biofilm was scanned using a systematic uniformly random sampling method (see description of the stereological analysis), and *z* series of optical sections were generated by vertical sectioning at 0.5 μm distances through the biofilm. This interval was chosen in order to include the major bacterial groups of supragingival biofilm.

Image analysis. Image analysis was performed using ImageJ 1.34s (Abramoff & Viergever, 2002; Rasband, 1997–2006). ImageJ was used to adjust output levels within the individual channels of the 24-bit RGB merged images. Prior to merging, the images for each colour channel were assembled into image stacks. In the merged images, streptococci, *A. naeslundii* and remaining bacteria were represented by green (yellow), blue (purple) and red colours, respectively. No other manipulation of the images was performed. For illustration purposes, maximum projection images of the entire confocal image stack were made for some 6 h, 12 h and 24 h specimens to compensate for the glass surfaces not being oriented completely parallel to the optical section plane.

Stereological analysis

Systematic uniformly random sampling. Stereological analysis was performed as a systematic uniformly random sampling of fields of view (Gundersen & Jensen, 1987) as previously described by Dige *et al.* (2009). First, the area of interest for estimating the number of bacteria present was identified as a 2×2 mm^2 quadrant in the centre of each glass slab in order to capture typical smooth surface biofilm. Subsequently, based on a visual inspection of the density of bacteria, four or eight systematic uniformly random sampling fields were chosen. The first field of view was sampled using a random number table. From this random starting point within the area of interest, the remaining three or seven fields of view were sampled by moving the microscope stage with a fixed *x* and *y* distance from the previous field (in this case 1000 μm in the *x*-axis and 500 or 1000 in the *y*-axis, depending on whether four or eight sampling fields were chosen). The principle of counting has been previously described (Dige *et al.*, 2009).

Quantification of bacteria. The number $\mathbf{Q}^-$ of bacteria was counted using the unbiased counting frame originally described by Gundersen (1977) and applied to bacteria, as described by Dige *et al.* (2009). The unbiased counting frame was superimposed on the images and fixed in the same position throughout subsequent focal planes. Bacteria

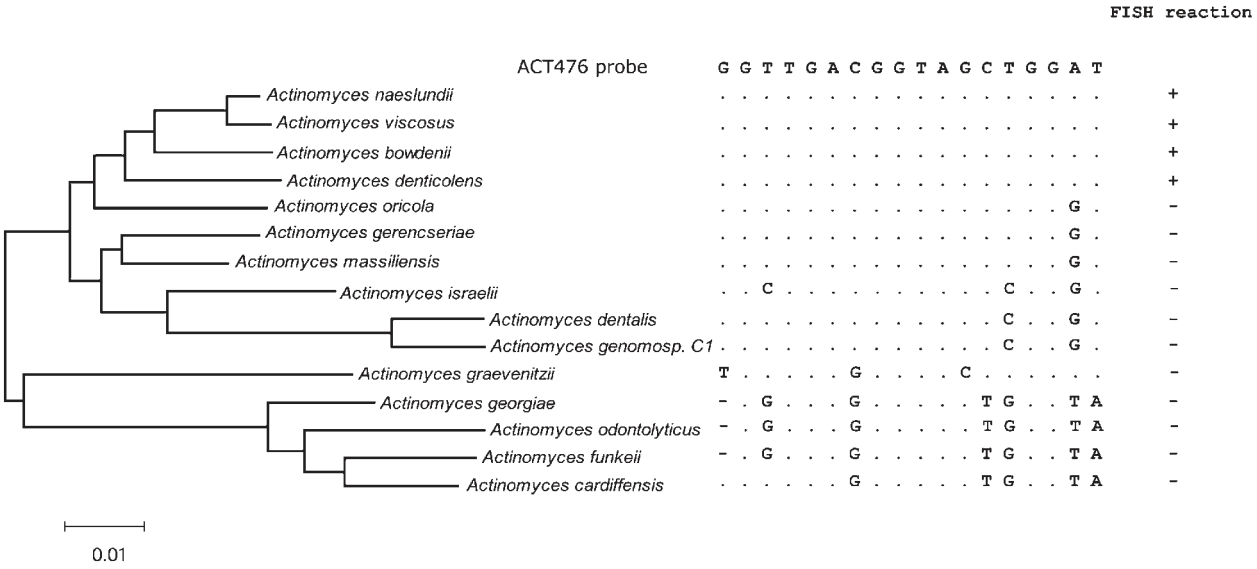

Fig. 1. Comparison of the target sequence of probe ACT476 in *Actinomyces* species shows that reactivity of the probe is restricted to members of the perfectly matching *A. naeslundii–A. viscosus–A. bowdeni–A. denticolens* cluster, among which only *A. naeslundii* is associated with humans. The phylogenetic tree of *Actinomyces* species shown to the left was based on complete 16S rRNA gene sequences clustered by the Minimum Evolution algorithm in MEGA version 4 (Tamura *et al.*, 2007).

were only counted the first time they came into focus in a section. Bacteria were counted manually, and to remember which bacteria had already been counted, the point picker in the Particle Analysis plugin in the ImageJ software was used. The software also maintained a record of the number of cell markers placed by the operator. Because of the pleomorphic morphology of ACT476-labelled bacteria the following counting rules were adopted: (i) for overlapping bacteria (intense fluorescence) the bacteria were counted as separate bacteria; (ii) when a space or a notch was observed, bacteria were counted as separate bacteria; (iii) bacteria showing a change in angle were counted as separate bacteria (Fig. 2). ACT476-labelled bacteria were counted on images of the blue channel only (with the other channels off), because of better differentiation when they were not intermingled with other types of bacteria (compare Fig. 4g and h). The principle for counting streptococci in division was to count them as two bacteria when the length was equal to that of two separate cocci.

The size and number of the unbiased counting frame varied according to cell density. For example, in specimens with low cell density (6 and 12 h), one counting frame was used covering the whole image except the outermost borders. On the other hand, when the cell density was high (multilayered biofilms) four counting frames of smaller areas were superimposed on the images. The strategy was such that for each specimen, approximately 100–200 bacteria needed to be counted to get reliable quantitative data (Gundersen *et al.*, 1999; Nyengaard, 1999). The dimensions of the counting frame(s) remained the same for all four/eight images in one specimen.

The raw counts of streptococci, *A. naeslundii* and remaining bacteria were used to estimate the total bacterial number within the area of interest (2×2 mm^2). Subsequently, the total number of bacteria for each glass slab, *N*, was estimated by the 2D fractionator (Dige *et al.*, 2009; Gundersen, 1986). For each volunteer two glass slabs were analysed at each time point and the mean value of the estimates was calculated.

Statistics. For each bacterial group the number of bacteria was plotted as a function of time on log-linear and log-log scales and evaluated for linear behaviour, signifying single-exponential or nonlinear growth, respectively.

The total variation between individuals (CV_{tot}) was determined, as regards the number of streptococci, the number of *A. naeslundii* and the total number of bacteria. The error variance due to the stereological method (CE_{met}) was estimated as the counting noise (Nyengaard, 1999), disregarding the error variance due to systematic sampling of sections and fields of view. The observed total variation [CV_{tot}=standard deviation (SD) divided by the mean] was calculated. From the CV_{tot} and the CE_{met}, the biological variation, CV_{bio}, was determined using the equation $CV^2_{tot} = CV^2_{bio} + CE^2_{met}$. Because the error variance due to the stereological method (CE_{met}) was very small (Dige *et al.*, 2009) the total variation between individuals (CV_{tot}) in the number of bacteria, as regards streptococci, *A. naeslundi* and total bacteria, was determined mainly by the biological variation (CV_{bio}). Calculation of the ratios of CE^2/CV^2_{tot} gave very small values, suggesting that a sufficient number of bacteria was counted (Nyengaard, 1999).

RESULTS

Quantitative observations

Fig. 3(a) shows the number of streptococci (green) and the number of *A. naeslundii* (blue) in biofilms developed during 6, 12, 24 and 48 h from the ten individuals. The distribution of the number of streptococci and *A. naeslundii* for the ten individuals is further illustrated in Supplementary Fig. S1 (available with the online version of this paper) by pairs of data with coloured lines. The speed of bacterial surface coverage varied considerably between individuals at all time points, but for both bacterial groups there was a notable increase in the number of bacteria over the observation period. A plot (Fig. 3b) of the slopes for the increase in ln(number of streptococci) versus the slopes for the increase in ln(number of *A. naeslundii*), evaluated as a function of increase in ln(time), showed a tendency towards a faster increase for streptococci than for *A. naeslundii*, although this was not statistically significant (paired *t*-test, $P=0.07$). This trend was supported by an analysis of changes in the proportion of bacteria between 6 and 48 h, which showed that in nine of the ten individuals there was a tendency to an increase in the proportion of streptococci relative to total bacteria, whereas the proportion of *A. naeslundii* decreased slightly or remained stable in nine of the ten individuals (Fig. 3c, d).

Qualitative observations

At 6 and 12 h, bacteria were scattered randomly across the surface, as single bacteria or as mono- and multi-genera

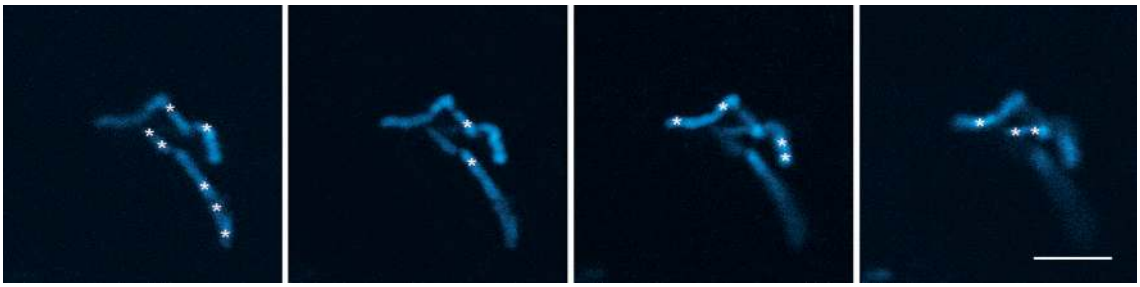

Fig. 2. Illustration of the principle of counting ACT476-labelled bacteria. The figure shows four consecutive *x-y* sections of 6 h biofilm on images of the blue channel only (with the other channels off), demonstrating *A. naeslundii* (blue). Bacteria were only counted the first time they came into focus in a section, as indicated by white * in the consecutive sections. For detailed explanation of the counting principle, see text. Scale bar, 5 μm.

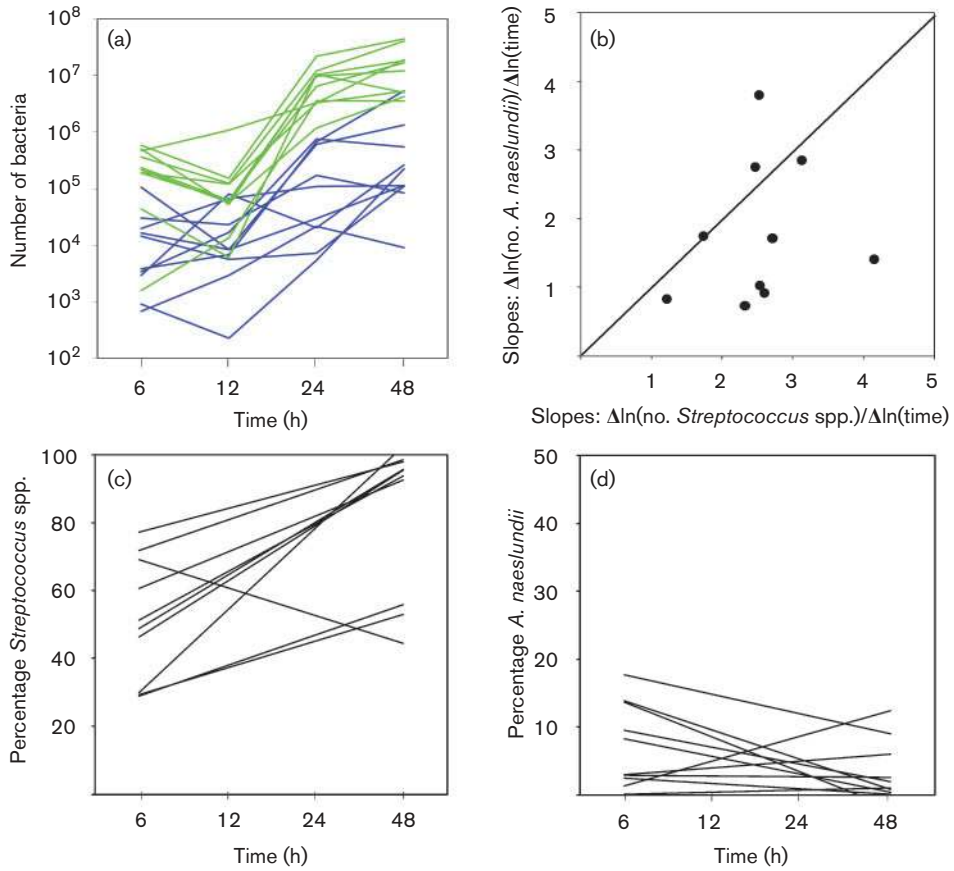

Fig. 3. (a) The number of *Streptococcus* spp. (green) (Dige *et al.*, 2009) and the number of *A. naeslundii* (blue) recorded in dental biofilms developed within 6, 12, 24 and 48 h in ten individuals. Note the logarithmic scale on the *y*-axis. The estimated numbers refer to a well-defined reference space that corresponds to an area of 4 mm^2. (b) The relationship between the slopes for the increase in number of streptococci versus the slopes for the increase in ln(number of *A. naeslundii*), evaluated as a function of the increase in ln(time), showing a tendency towards a faster increase for streptococci than for *A. naeslundii.* However, this was not statistically significant (paired *t*-test, $P=0.07$). The bold line indicates an equal slope for the increase in number of *A. naeslundii* and streptococci. (c, d) Linear association (trend lines) of the changes in the proportion of *Streptococcus* spp. (c) and *A. naeslundii* (d) as a percentage of the total number of bacteria between 6 and 48 h in ten individuals. Note different scales on the *y*-axis in (c) and (d).

clusters of bacteria, many of which appeared in a stage of cell division (Fig. 4a–e). In all individuals *A. naeslundii* was observed at all time points scattered throughout the biofilm. In the early stages *A. naeslundii* was in all individuals recorded as single coccoid rods or short rods arranged in Y, V and T shapes (Fig. 4a, b, d), and in six of the ten individuals also as longer rods or filamentous bacteria (Fig. 4a, c, e). *A. naeslundii* was observed both as isolated clusters (Fig. 4a, c) and in mixed clusters with streptococci and/or other bacteria (Fig. 4a, d, e). Notable differences in the amount of bacteria and the composition of the microbiota were observed both across the experimental surface and between surfaces carried by different individuals.

At 24 h and 48 h, the biofilm showed dominance of streptococci (Figs 4f, g and 5b). Three individuals, in addition, showed large accumulations of non-streptococci (Fig. 5a), including *A. naeslundii* and large coccoid non-streptococci in pairs or tetrads. Eight of the ten individuals showed *A. naeslundii* arranged in microcolonies of varying size consisting of branching filaments, some of which were 'spider colonies' consisting of branching filaments radiating from a single point (Fig. 4f, g, h). *A. naeslundii* was also observed intermingling with streptococci and other non-streptococci in most individuals (Fig. 4f, g). Also at these more advanced stages of biofilm formation the pattern and degree of microbial coverage, as well as the thickness of the biofilm, varied within and between individuals from incomplete (Fig. 4f) to complete surface coverage by bacteria (Fig. 4g), in some parts with prominences ('chimneys') of multilayered complex microcolonies (Figs 5 and 6). All types of bacteria showed various stages of cell division reflected by their pair-wise (Fig. 4f) or branching arrangement (Fig. 4f, h).

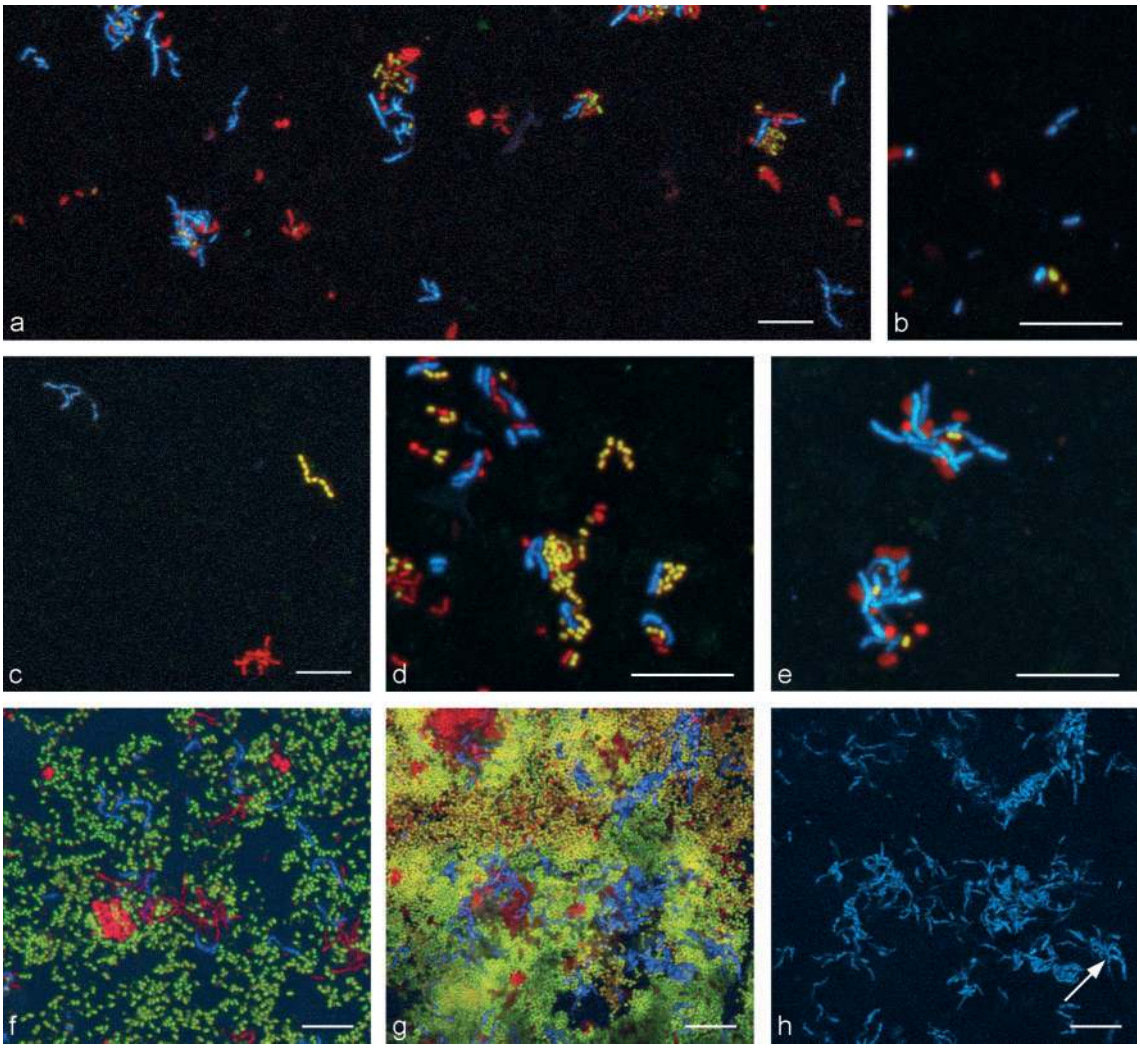

Fig. 4. CLSM images of *in situ* biofilm on glass surfaces (*x-y* sections). Biofilms were stained simultaneously with all-bacterium-specific EUB338 probe, *Streptococcus*-specific STR405 probe and *Actinomyces*-specific ACT476 probe. Green (yellow), blue (purple) and red represent streptococci, *A. naeslundii* and the remaining bacteria, respectively. (a–e) Images of the microbial colonization pattern after 6 h (a, d, e) and 12 h (b, c) in four different individuals, showing solitary bacteria and bacteria in clusters. *A. naeslundii* was observed as single bacteria (b) and in isolated clusters (a, c) as well as in mixed clusters with other bacteria (a, d, e). (f, g) 24 h biofilms from two different individuals. Note marked differences in the degree of microbial coverage. In all cases the biofilms consist predominantly of streptococci. (h) ACT476-labelled bacteria from (g) as revealed by the blue channel only. *A. naeslundii* cells are arranged in microcolonies of varying sizes consisting of branching filaments or as 'spider colonies' (arrow). Panels (a–f) are maximum projection images; (g, h) are optical *x-y* sections ~2 μm from the supporting surface. Scale bar for all images, 10 μm.

Examination of the biofilms in the *z*-axis (*x-y* sections parallel to the surface) allowed a detailed analysis of the central parts of the 'chimneys'. The central parts of the 'chimneys' varied in composition and were either sparsely colonized (Figs 5b and 6b) or composed of non-streptococci (Figs 5a and 6a), including large coccoid bacteria, *A. naeslundii*, other rod-shaped/filamentous bacteria, or other non-streptococci and non-*A. naeslundii*. Analyses along the *z*-axis further demonstrated that, at the surface of the multilayered biofilms, bacteria of different genera regularly co-localized.

Analysis of consecutive sections of the multilayered biofilm parallel to the surface showed that *A. naeslundii* predominantly colonized the inner part next to the glass surface, and was more sparsely distributed in the outer layers (Fig. 5). Some *A. naeslundii* microcolonies extended perpendicularly from the supporting surface surrounded by other bacteria and forming 'chimney structures'. Sagittal (*x-z*, *y-z*) sections confirmed the presence of *A. naeslundii* in the inner layers as individual pleomorphic bacteria were oriented at different angles to the surface and forming palisades (Fig. 6).

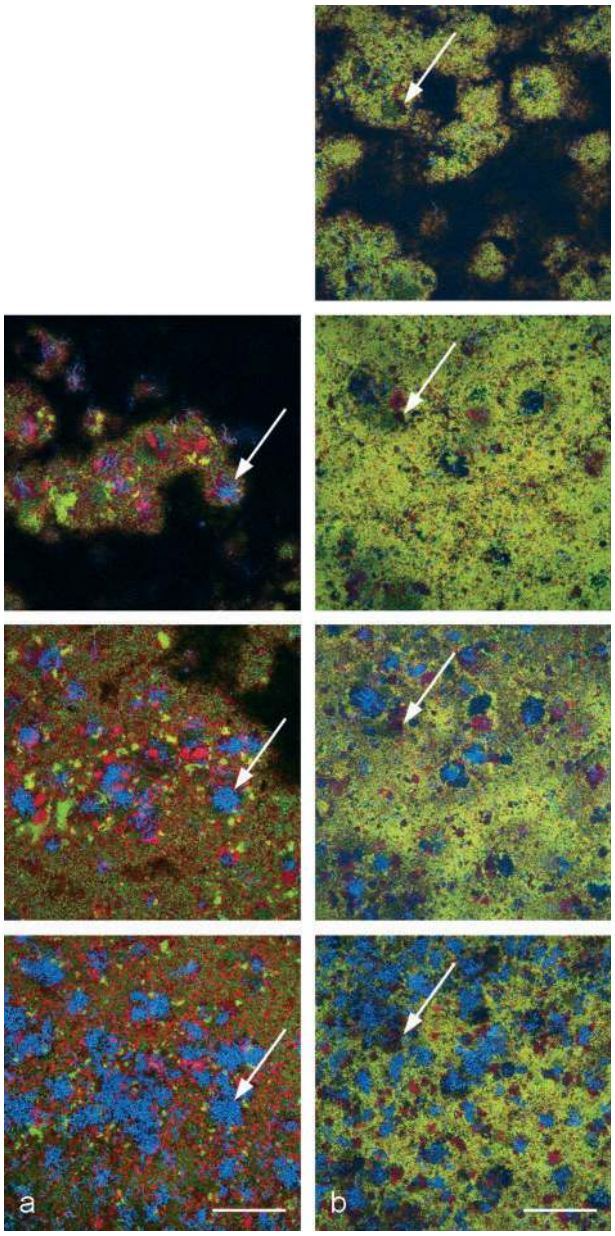

Fig. 5. CLSM images of 48 h *in situ* biofilm showing consecutive *x-y* sections at 4 μm intervals (along the *z*-axis) from the supporting glass surface (bottom image) in two different individuals. Biofilms were stained simultaneously with all-bacterium-specific EUB338 probe, *Streptococcus*-specific STR405 probe and *Actinomyces*-specific ACT476 probe. Green (yellow), blue (purple) and red represent represent streptococci, *A. naeslundii* and the remaining bacteria, respectively. *A. naeslundii* (purple-blue) are predominantly located in the inner part next to the glass surface, whereas these species are more sparsely distributed in the outer layers. In both illustrations columnar microcolonies protrude as circular projections (chimneys) at varying distances from the supporting surface. In (a) the central part of the microcolonies is composed of *A. naeslundii* (arrows) or other non-streptococci whereas in (b) the central parts are often sparsely colonized (arrows). Scale bar for all images, 50 μm.

DISCUSSION

Several *Actinomyces* species belong to the resident oral microbiota of supra-gingival plaque, although studies based on culture, checkerboard hybridization, 16S rRNA gene libraries and FISH reveal significant differences in their proportions depending on the age of the biofilm (Al-Ahmad *et al.*, 2007; Diaz *et al.*, 2006; Haffajee *et al.*, 2008; Li *et al.*, 2004; Ramberg *et al.*, 2003). Using a species-specific oligonucleotide probe this study confirms the checkerboard hybridization-based demonstration of *A. naeslundii* as a significant member of the initial colonizers of tooth surfaces. For the first time, our study provides a presentation of the spatio-temporal organization of *A. naeslundii* in relation to other bacteria in initial multi-layer dental biofilms formed *in vivo* up to 48 h and definitively demonstrates that *A. naeslundii* preferentially occupies the inner part of early multilayered biofilms. We therefore infer that the densely packed, pleomorphic Gram-positive bacteria with thick cell walls previously observed close to the enamel surface in electron micrographs (Listgarten *et al.*, 1975; Nyvad & Fejerskov, 1987b; Schroeder & De Boever, 1970) are *A. naeslundii*.

A. naeslundii was often observed in mixed clusters with streptococci and other bacteria at 6 and 12 h. This observation supports the view that co-adhesion, in particular co-adhesion processes involving *A. naeslundii*, streptococci and other bacteria, play an important role during the initial stages of colonization of tooth surfaces (Bos *et al.*, 1996; Gibbons & Nygaard, 1970; Kolenbrander, 1988; Kolenbrander *et al.*, 1990; Palmer *et al.*, 2003; Yoshida *et al.*, 2006). This observation is further supported by the finding of genotypically different bacteria co-localizing at the outer surface of the biofilm, indicating that co-adhesion of bacteria from saliva is a continuing process adding to the biomass of the developing biofilm. However, it is conceivable that cell division is the major contributor to the rapid increase in biomass during the first 24–48 h of biofilm formation, as suggested by several reports (Bloomquist *et al.*, 1996; Skopek *et al.*, 1993; Ørstavik, 1984). This is in line with the results of the present study, in which many bacteria appeared in a stage of cell division, including *A. naeslundii*, which formed branching filaments or 'spider colonies'. Likewise, it is conceivable that the decrease in the relative proportion of *A. naeslundii* between 6 and 48 h of biofilm formation observed in this and previous studies (Al-Ahmad *et al.*, 2007; Li *et al.*, 2004) reflects the effect of cell division and is a direct result of slower cell division of *A. naeslundii* relative to streptococci and other members of the microbiota. Similar shifts in the relative composition of the microbiota have been recorded during biofilm formation in experimental rats (Beckers & van der Hoeven, 1984).

The observation of densely packed colonies of *A. naeslundii* in the innermost part of the biofilm adjacent to the supporting surface has interesting ecological implications.

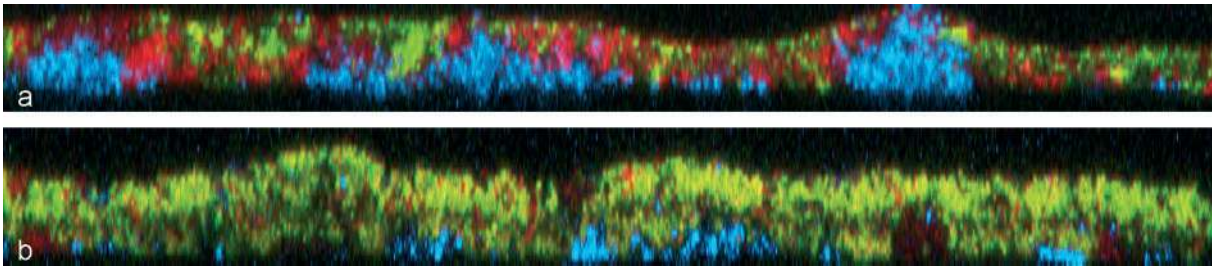

Fig. 6. CLSM images of 48 h *in situ* biofilm showing sagittal (*x*-*z*, *y*-*z*) sections of specimens from each of the two individuals shown in Fig. 5. Note that *A. naeslundii* (blue) are predominantly identified in the inner part next to the glass surface. Some microcolonies of *A. naeslundii* extended almost throughout the entire thickness of the biofilm (a). Note also sparsely colonized zones next to the supporting surface (b). The width of both images is 200 μm, and the heights of the images are 18 μm and 23 μm, respectively.

In contrast to streptococci, *A. naeslundii* has a unique glycolytic system in which the bacteria use phosphoryl donors instead of ATP for carbohydrate degradation (Takahashi *et al.*, 1995). *Actinomyces* species can use lactate as a carbon source for growth (Takahashi & Yamada, 1996; van der Hoeven & van den Kieboom, 1990), whereby lactic acid is converted into weaker acids (Takahashi & Yamada, 1996). A pH-modulating activity of these species may, theoretically, occur also via degradation of urea (Yaling *et al.*, 2006). Moreover, through its metabolism, *Actinomyces* species can remove oxygen from the environment and create an anaerobic milieu (Takahashi & Yamada, 1996), suitable for outgrowth of some other bacteria. Finally, recent observations demonstrate that co-aggregation with *A. naeslundii* stabilizes arginine metabolism in *Streptococcus gordonii* and reduces its dependence on extracellular arginine, which is a limiting factor in the environment of the early colonizers (Jakubovics *et al.*, 2008; Van Wuyckhuyse *et al.*, 1995). Collectively, these properties make *A. naeslundii* an essential initial colonizer of tooth surfaces and particularly well adapted to live and survive in substrate-limited environments deep in the biofilm. The concerted metabolic activities of these bacteria may have a controlling effect on dental caries processes by reducing the acidogenic potential of the biofilm (Takahashi & Nyvad, 2008).

With increasing age of the biofilm, microcolonies of *A. naeslundii* and other non-streptococci were seen to extend perpendicularly from the supporting surface as 'chimney' structures and palisades like those observed by electron microscopy of multi-layered dental plaque (Listgarten *et al.*, 1975; Nyvad & Fejerskov, 1987b; Rosan *et al.*, 1976). The morphogenesis of these particular structures can only be speculated on. It may reflect a constrained physical environment during development of the biofilm whereby overgrowth of rapidly multiplying species may hinder the growth of other bacteria with a lower growth rate such as *Actinomyces* species. Alternatively or additionally, such structures may result from nutritional interrelationships between different microbial species or specific co-adhesion/co-aggregation processes. Thus, Bos *et al.* (1996) proposed that streptococci may encapsulate *Actinomyces* to form micro-anaerobic domains in the biofilm, which are needed for optimal growth of the *Actinomyces*. This hypothesis corroborates more recent concepts of bacterial multicellularity that bacteria growing in biofilm communities have communication and decision-making capabilities that enable them to coordinate growth and biochemical activities (Jakubovics *et al.*, 2008; for reviews see Kolenbrander *et al.*, 2006; Shapiro, 1998). Hence, it has been suggested that the growth rate of adherent cells is enhanced when a certain cell density is reached, whereas the growth rate drops at higher densities. This density-dependent growth may be explained by cell–cell signalling, resulting in physical or morphological changes of the biofilm bacteria (Bloomquist *et al.*, 1996).

In this study, *A. naeslundii* represented a large spectrum of morphotypes, ranging from coccoid to small rods and filamentous bacteria. It has been suggested previously that *A. naeslundii* exhibits pleomorphism, the coccoid form predominating during the early stages, whereas rod-shaped or filamentous forms become prominent after 24–48 h (Nyvad & Fejerskov, 1987b). This observation is consistent with our study (compare Fig. 4b with Fig. 4f, h) as well as immunoelectron microscopic studies of dental plaque *in situ,* in which *A. viscosus* (*A. naeslundii* according to present nomenclature) tended to be cocco-bacillary in the superficial layers and filamentous in the deeper layers (Berthold *et al.*, 1982).

The observation of sparsely colonized areas in the centre of the circular projections and deeper parts of multilayered biofilms (Fig. 5) is open for speculation. Such unstained regions have been suggested to represent open voids (Pratten *et al.*, 2000; Wood *et al.*, 2000) or to contain extracellular polysaccharides (Thurnheer *et al.*, 2004). However, one cannot exclude the possibility that these areas contain bacteria labelled with dyes that are bleached away by out-of-focus excitation during the consecutive scanning through the biofilm, or bacteria exhibiting

insufficient fluorescent signals because of low rRNA content due to slow growth or low metabolic state (Amann *et al.*, 1995; Hannig *et al.*, 2007; Moter & Göbel, 2000; Schuppler *et al.*, 1998). In fact, in some instances we found the fluorescent signal of the ACT476 probe to be bright, whereas the signal of the EUB338 probe of the same bacteria was very low or absent. Of particular relevance to our stereological approach, it has been previously observed that the *in situ* hybridization of Gram-positive filamentous bacteria such as *Actinomyces* often results in an irregular distribution of fluorescent signals over the whole filaments (Schuppler *et al.*, 1998), possibly because of insufficient permeability of the bacterial cell walls, which has been documented also for actinomycetes in other ecosystems (Müller *et al.*, 2007; Schuppler *et al.*, 1998). Consequently underestimation of the number of some bacteria cannot be excluded (Dige *et al.*, 2009).

In conclusion, by combining qualitative and quantitative methods this study resulted in new insight into the temporo-spatial relationships as well as the population dynamics of *A. naeslundii* relative to streptococci in the initial phases of biofilm formation on oral solid non-shedding surfaces. A remarkable observation of the study was the preferential colonization of *A. naeslundii* in the deeper regions of the biofilm. In view of the pH-modulating properties of *A. naeslundii* it is relevant to further explore the ecological role of this species in the processes of dental caries.

ACKNOWLEDGEMENTS

The authors thank Dr R. Gmür (Institute of Oral Biology, University of Zürich, Switzerland) for helpful suggestions and discussion regarding oligonucleotide ACT476. We gratefully acknowledge the statistical advice by Dr V. Bælum (School of Dentistry, Aarhus University, Denmark) and Dr M. Væth (Department of Biostatistics, Aarhus University, Denmark). Special gratitude is extended to laboratory technician A. Larsen for technical assistance with the CLSM work and laboratory technician L. Grønkjær for technical assistance with the application of the FISH procedures. This work was supported by Aarhus University Research Foundation, the Swedish Patent Revenue Fund for Research in Preventive Odontology, and the Danish Dental Association. J. R. N. and M. K. R. were supported by the Lundbeck Foundation and the Danish Council for Strategic Research.

REFERENCES

Abramoff, M. D. & Viergever, M. A. (2002). Computation and visualization of three-dimensional soft tissue motion in the orbit. *IEEE Trans Med Imaging* **21**, 296–304.

Al-Ahmad, A., Wunder, A., Auschill, T. M., Follo, M., Braun, G., Hellwig, E. & Arweiler, N. B. (2007). The *in vivo* dynamics of *Streptococcus* spp., *Actinomyces naeslundii*, *Fusobacterium nucleatum* and *Veillonella* spp. in dental plaque biofilm as analysed by five-colour multiplex fluorescence *in situ* hybridization. *J Med Microbiol* **56**, 681–687.

Amann, R. I., Binder, B. J., Olson, R. J., Chisholm, S. W., Devereux, R. & Stahl, D. A. (1990). Combination of 16S rRNA-targeted oligonucleotide probes with flow cytometry for analyzing mixed microbial populations. *Appl Environ Microbiol* **56**, 1919–1925.

Amann, R. I., Ludwig, W. & Schleifer, K. H. (1995). Phylogenetic identification and in situ detection of individual microbial cells without cultivation. *Microbiol Rev* **59**, 143–169.

Anwar, H., Strap, J. L. & Costerton, J. W. (1992). Establishment of aging biofilms: possible mechanism of bacterial resistance to antimicrobial therapy. *Antimicrob Agents Chemother* **36**, 1347–1351.

Auschill, T. M., Hellwig, E., Sculean, A., Hein, N. & Arweiler, N. B. (2004). Impact of the intraoral location on the rate of biofilm growth. *Clin Oral Investig* **8**, 97–101.

Beckers, H. J. & van der Hoeven, J. S. (1984). The effects of mutual interaction and host diet on the growth rates of the bacteria *Actinomyces viscosus* and *Streptococcus mutans* during colonization of tooth surfaces in di-associated gnotobiotic rats. *Arch Oral Biol* **29**, 231–236.

Berthold, P., Lai, C. H. & Listgarten, M. A. (1982). Immunoelectron microscopic studies of *Actinomyces viscosus*. *J Periodontal Res* **17**, 26–40.

Bloomquist, C. G., Reilly, B. E. & Liljemark, W. F. (1996). Adherence, accumulation, and cell division of a natural adherent bacterial population. *J Bacteriol* **178**, 1172–1177.

Bos, R., van der Mei, H. C. & Busscher, H. J. (1996). Co-adhesion of oral microbial pairs under flow in the presence of saliva and lactose. *J Dent Res* **75**, 809–815.

Costerton, J. W., Cook, G. & Lamont, R. (1999). The community architecture of biofilms: dynamic structures and mechanisms. In *Dental Plaque Revisited. Oral Biofilms in Health and Disease,* pp. 5–14. Edited by H. N. Newman & M. Wilson. Cardiff, UK: Bioline.

Daims, H., Bruhl, A., Amann, R., Schleifer, K. H. & Wagner, M. (1999). The domain-specific probe EUB338 is insufficient for the detection of all bacteria: development and evaluation of a more comprehensive probe set. *Syst Appl Microbiol* **22**, 434–444.

Davies, D. (2003). Understanding biofilm resistance to antibacterial agents. *Nat Rev Drug Discov* **2**, 114–122.

Diaz, P. I., Chalmers, N. I., Rickard, A. H., Kong, C., Milburn, C. L., Palmer, R. J., Jr & Kolenbrander, P. E. (2006). Molecular characterization of subject-specific oral microflora during initial colonization of enamel. *Appl Environ Microbiol* **72**, 2837–2848.

Dige, I., Nilsson, H., Kilian, M. & Nyvad, B. (2007). *In situ* identification of streptococci and other bacteria in initial dental biofilm by confocal laser scanning microscopy and fluorescence *in situ* hybridization. *Eur J Oral Sci* **115**, 459–467.

Dige, I., Nyengaard, J. R., Kilian, M. & Nyvad, B. (2009). Application of stereological principles for quantification of bacteria in intact dental biofilms. *Oral Microbiol Immunol* **24**, 69–75.

DuPont, G. A. (1997). Understanding dental plaque; biofilm dynamics. *J Vet Dent* **14**, 91–94.

Gibbons, R. J. & Nygaard, M. (1970). Interbacterial aggregation of plaque bacteria. *Arch Oral Biol* **15**, 1397–1400.

Gmür, R. & Lüthi-Schaller, H. (2007). A combined immunofluorescence and fluorescent in situ hybridization assay for single cell analyses of dental plaque microorganisms. *J Microbiol Methods* **69**, 402–405.

Gundersen, H. J. (1977). Notes on the estimation of the numerical density of arbitrary profiles: the edge effect. *J Microsc* **111**, 219–223.

Gundersen, H. J. (1986). Stereology of arbitrary particles. A review of unbiased number and size estimators and the presentation of some new ones, in memory of William R. Thompson. *J Microsc* **143**, 3–45.

Gundersen, H. J. & Jensen, E. B. (1987). The efficiency of systematic sampling in stereology and its prediction. *J Microsc* **147**, 229–263.

Gundersen, H. J., Jensen, E. B., Kieu, K. & Nielsen, J. (1999). The efficiency of systematic sampling in stereology – reconsidered. *J Microsc* **193**, 199–211.

Haffajee, A. D., Socransky, S. S., Patel, M. R. & Song, X. (2008). Microbial complexes in supragingival plaque. *Oral Microbiol Immunol* **23**, 196–205.

Hannig, C., Hannig, M., Rehmer, O., Braun, G., Hellwig, E. & Al-Ahmad, A. (2007). Fluorescence microscopic visualization and quantification of initial bacterial colonization on enamel *in situ*. *Arch Oral Biol* **52**, 1048–1056.

Jakubovics, N. S., Gill, S. R., Iobst, S. E., Vickerman, M. M. & Kolenbrander, P. E. (2008). Regulation of gene expression in a mixed-genus community: stabilized arginine biosynthesis in *Streptococcus gordonii* by coaggregation with *Actinomyces naeslundii*. *J Bacteriol* **190**, 3646–3657.

Kilian, M., Larsen, M. J., Fejerskov, O. & Thylstrup, A. (1979). Effects of fluoride on the initial colonization of teeth *in vivo*. *Caries Res* **13**, 319–329.

Kolenbrander, P. E. (1988). Intergeneric coaggregation among human oral bacteria and ecology of dental plaque. *Annu Rev Microbiol* **42**, 627–656.

Kolenbrander, P. E., Andersen, R. N. & Moore, L. V. (1990). Intrageneric coaggregation among strains of human oral bacteria: potential role in primary colonization of the tooth surface. *Appl Environ Microbiol* **56**, 3890–3894.

Kolenbrander, P. E., Palmer, R. J., Jr, Rickard, A. H., Jakubovics, N. S., Chalmers, N. I. & Diaz, P. I. (2006). Bacterial interactions and successions during plaque development. *Periodontol 2000* **42**, 47–79.

Li, J., Helmerhorst, E. J., Leone, C. W., Troxler, R. F., Yaskell, T., Haffajee, A. D., Socransky, S. S. & Oppenheim, F. G. (2004). Identification of early microbial colonizers in human dental biofilm. *J Appl Microbiol* **97**, 1311–1318.

Listgarten, M. A., Mayo, H. E. & Tremblay, R. (1975). Development of dental plaque on epoxy resin crowns in man. A light and electron microscopic study. *J Periodontol* **46**, 10–26.

Moter, A. & Göbel, U. B. (2000). Fluorescence in situ hybridization (FISH) for direct visualization of microorganisms. *J Microbiol Methods* **41**, 85–112.

Müller, E., Schade, M. & Lemmer, H. (2007). Filamentous scum bacteria in activated sludge plants: detection and identification quality by conventional activated sludge microscopy versus fluorescence *in situ* hybridization. *Water Environ Res* **79**, 2274–2286.

Nyengaard, J. R. (1999). Stereologic methods and their application in kidney research. *J Am Soc Nephrol* **10**, 1100–1123.

Nyvad, B. & Fejerskov, O. (1987a). Scanning electron microscopy of early microbial colonization of human enamel and root surfaces *in vivo*. *Scand J Dent Res* **95**, 287–296.

Nyvad, B. & Fejerskov, O. (1987b). Transmission electron microscopy of early microbial colonization of human enamel and root surfaces *in vivo*. *Scand J Dent Res* **95**, 297–307.

Nyvad, B. & Fejerskov, O. (1989). Structure of dental plaque and the plaque-enamel interface in human experimental caries. *Caries Res* **23**, 151–158.

Nyvad, B. & Kilian, M. (1987). Microbiology of the early colonization of human enamel and root surfaces *in vivo*. *Scand J Dent Res* **95**, 369–380.

Nyvad, B. & Kilian, M. (1990). Microflora associated with experimental root surface caries in humans. *Infect Immun* **58**, 1628–1633.

Ørstavik, D. (1984). Initial bacterial adhesion to surfaces: ecological implications in dental plaque formation. In *Bacterial Adhesion and Preventive Dentistry*, pp. 153–166. Edited by J. M. ten Cate, S. A. Leach & J. Arends. Washington, DC: IRL Press.

Palmer, R. J., Gordon, S. M., Cisar, J. O. & Kolenbrander, P. E. (2003). Coaggregation-mediated interactions of streptococci and actinomyces detected in initial human dental plaque. *J Bacteriol* **185**, 3400–3409.

Paster, B. J., Bartoszyk, I. M. & Dewhirst, F. E. (1998). Identification of oral streptococci using PCR-based, reverse-capture, checkerboard hybridization. *Methods Cell Sci* **20**, 223–231.

Pratten, J., Andrews, C. S., Craig, D. Q. & Wilson, M. (2000). Structural studies of microcosm dental plaques grown under different nutritional conditions. *FEMS Microbiol Lett* **189**, 215–218.

Ramberg, P., Sekino, S., Uzel, N. G., Socransky, S. & Lindhe, J. (2003). Bacterial colonization during de novo plaque formation. *J Clin Periodontol* **30**, 990–995.

Rasband, W. S. (1997–2006). ImageJ. US National Institutes of Health, Bethesda, Maryland, USA, http://rsb.info.nih.gov/ij/. **1.34s**.

Ritz, H. L. (1967). Microbial population shifts in developing human dental plaque. *Arch Oral Biol* **12**, 1561–1568.

Rosan, B., Lai, C. H. & Listgarten, M. A. (1976). *Streptococcus sanguis*: a model in the application in immunochemical analysis for the in situ localization of bacteria in dental plaque. *J Dent Res* **55**, A124–A141.

Schroeder, H. E. & De Boever, J. A. (1970). The structure of microbial dental plaque. In *Dental Plaque*, pp. 49–70. Edited by W. D. McHugh. Dundee: C.D. Thomson & Co.

Schuppler, M., Wagner, M., Schön, G. & Göbel, U. B. (1998). *In situ* identification of nocardioform actinomycetes in activated sludge using fluorescent rRNA-targeted oligonucleotide probes. *Microbiology* **144**, 249–259.

Shapiro, J. A. (1998). Thinking about bacterial populations as multicellular organisms. *Annu Rev Microbiol* **52**, 81–104.

Skopek, R. J., Liljemark, W. F., Bloomquist, C. G. & Rudney, J. D. (1993). Dental plaque development on defined streptococcal surfaces. *Oral Microbiol Immunol* **8**, 16–23.

Socransky, S. S., Manganiello, A. D., Propas, D., Oram, V. & van Houte, J. (1977). Bacteriological studies of developing supragingival dental plaque. *J Periodontal Res* **12**, 90–106.

Stahl, D. A. & Amann, R. (1991). Development and application of nucleic acid probes. In *Nucleic Acid Techniques in Bacterial Systematics*, 1st edn, pp. 205–248. Edited by E. Stackebrandt & M. Goodfellow. Chichester, UK: Wiley.

Syed, S. A. & Loesche, W. J. (1978). Bacteriology of human experimental gingivitis: effect of plaque age. *Infect Immun* **21**, 821–829.

Takahashi, N. & Nyvad, B. (2008). Caries ecology revisited: microbial dynamics and the caries process. *Caries Res* **42**, 409–418.

Takahashi, N. & Yamada, T. (1996). Catabolic pathway for aerobic degradation of lactate by *Actinomyces naeslundii*. *Oral Microbiol Immunol* **11**, 193–198.

Takahashi, N., Kalfas, S. & Yamada, T. (1995). Phosphorylating enzymes involved in glucose fermentation of *Actinomyces naeslundii*. *J Bacteriol* **177**, 5806–5811.

Tamura, K., Dudley, J., Nei, M. & Kumar, S. (2007). MEGA4: Molecular Evolutionary Genetics Analysis (MEGA) software version 4.0. *Mol Biol Evol* **24**, 1596–1599.

Thurnheer, T., Gmür, R. & Guggenheim, B. (2004). Multiplex FISH analysis of a six-species bacterial biofilm. *J Microbiol Methods* **56**, 37–47.

van der Hoeven, J. S. & van den Kieboom, C. W. (1990). Oxygen-dependent lactate utilization by *Actinomyces viscosus* and *Actinomyces naeslundii*. *Oral Microbiol Immunol* **5**, 223–225.

van Palenstein Helderman, W. H. (1981). Longitudinal microbial changes in developing human supragingival and subgingival dental plague. *Arch Oral Biol* **26**, 7–12.

Van Wuyckhuyse, B. C., Perinpanayagam, H. E., Bevacqua, D., Raubertas, R. F., Billings, R. J., Bowen, W. H. & Tabak, L. A. (1995). Association of free arginine and lysine concentrations in human parotid saliva with caries experience. *J Dent Res* **74**, 686–690.

Wood, S. R., Kirkham, J., Marsh, P. D., Shore, R. C., Nattress, B. & Robinson, C. (2000). Architecture of intact natural human plaque biofilms studied by confocal laser scanning microscopy. *J Dent Res* **79**, 21–27.

Yaling, L., Tao, H., Jingyi, Z. & Xuedong, Z. (2006). Characterization of the *Actinomyces naeslundii* ureolysis and its role in bacterial aciduricity and capacity to modulate pH homeostasis. *Microbiol Res* **161**, 304–310.

Yoshida, Y., Palmer, R. J., Yang, J., Kolenbrander, P. E. & Cisar, J. O. (2006). Streptococcal receptor polysaccharides: recognition molecules for oral biofilm formation. *BMC Oral Health* **6** (*Suppl 1*), S12.

Edited by: P. Kolenbrander